Non-dipole photoemission effects in x-ray standing wavefield determination of surface structure

1998 J. Phys.: Condens. Matter 10 L623

(http://iopscience.iop.org/0953-8984/10/35/004)

J. Phys.: Condens. Matter **10** (1998) L623–L629. Printed in the UK PII: S0953-8984(98)96221-X

LETTER TO THE EDITOR

Non-dipole photoemission effects in x-ray standing wavefield determination of surface structure

C J Fisher†, R Ithin†, R G Jones†, G J Jackson‡, D P Woodruff‡ and B C C Cowie§

† Chemistry Department, University of Nottingham, Nottingham NG7 2RD, UK
‡ Physics Department, University of Warwick, Coventry CV4 7AL, UK
§ CCLRC Daresbury Laboratory, Warrington WA4 4AD, UK

Received 24 July 1998

Abstract. Non-dipolar effects in the angular distribution of core level photoemission are shown to have a substantial influence on the interpretation of x-ray standing wavefield determinations of surface adsorption structures when the x-ray absorption is monitored by photoemission, even at photon energies below 3 keV. Results for I adsorption on Cu(111) are shown to be compatible with theoretical calculations for atomic Xe.

It is widely recognized that the dipolar description of the photoemission process is a first-order approximation, but in using photoemission in solid state and surface science it is assumed that the associated photon energies are too low to allow quadrupole and magnetic dipole effects to be important. In this letter we show that the impact of these higher order terms in modifying the angular distribution of photoemission can actually be of considerable importance at rather soft x-ray energies (around 3 keV or lower), and show specifically that failure to account for them can lead to significant errors in surface structural parameters obtained from x-ray standing wave (XSW) measurements monitored by core level photoemission. More generally, the different angular distributions from different energy levels will impact on any surface measurement reliant on quantitative photoemission intensity comparisons.

The fact that non-dipole effects can strongly influence the angular dependence of core level photoemission, at far lower energies than the onset of comparable effects in the total photoionization cross-section, has been demonstrated experimentally rather recently for atomic Ar and Kr [1, 2], confirming earlier theoretical predictions [3]. In the dipole approximation the photoemitted intensity at a given angle to the photon propagation direction is independent of whether this is in the forward or backward direction, but a key feature of non-dipole contributions is that this symmetry is lost. It is this backward/forward asymmetry which makes the effect important in experiments involving x-ray standing waves in solids. A recent theoretical treatment of non-dipole effects in XSW considers explicitly only the influence on the integral photoelectron yield, estimated to be about 1% for our experiment [4]; by contrast, the effect we observe is some 60% signal enhancement.

In the XSW technique [5, 6], a Bragg reflection is excited in a solid and the interference of the incident and scattered x-ray waves gives rise to a standing wave, the nodal planes of which lie parallel to the Bragg scatterer planes while their spacing equals that of the scatterer planes. As one scans, in incidence angle or photon energy, through the finite

0953-8984/98/350623+07$19.50

range of reflectivity associated with this condition, the standing wavefield shifts in phase in a predictable fashion, and the lineshape of the x-ray absorption in this range at specific atoms provides a signature of their location relative to the bulk scatterer planes. This x-ray absorption can be monitored by detecting the x-ray fluorescence following the core-hole decay, but in surface structural studies it is often convenient, as well as more surface specific, to monitor this absorption via the Auger electron emission associated with core-hole decay, or more directly through the intensity of the associated photoemission. These latter methods are especially relevant for experiments involving Bragg reflections close to normal incidence to the scatterer planes [7] which occur at relatively soft x-ray energies (typically 2–5 keV). Photoemission monitoring offers the special advantage of chemical state sensitivity due to the photoelectron binding energy differences found in core level photoemission from atoms of the same elemental species in different bonding situations [8]. It also generally offers a superior signal to background ratio relative to Auger peak monitoring for low atomic number species having only shallow core levels.

Even in the dipole approximation, photoelectron detection of x-ray standing waves has been shown to be influenced by the photoelectron angular distribution when using an arbitrary incidence angle to the Bragg scatterer planes [9], but when the polarization vector lies parallel to the scatterer planes such photoemission does monitor x-ray absorption directly. This condition is met in normal incidence XSW (NIXSW) which has the added advantage of being rather insensitive to crystal imperfections (mosaicity). It can thus be applied to a wide range of conventionally-prepared single-crystal materials using a relatively low resolution synchrotron radiation beamline, albeit with some reduction in the amplitude of the measured XSW modulation [7]. XSW provides information on layer spacings relative to the scatterer planes, and the layer spacing perpendicular to the surface is of especial importance, so one condition which is invariably used in these experiments is that of normal incidence to the surface. In this geometry the electron detector necessarily collects electrons in the 'backward' direction relative to the incident photon propagation; i.e. with a velocity component in the opposite sense to that of the incident photon. On the other hand, this electron detector is in a 'forward' direction relative to the reflected x-rays which suffer 180° scattering. This means that if there is a backward/forward asymmetry in the photoemission due to non-dipole excitation, the measurement detects the incident and reflected x-ray components of the standing wave with different efficiency, leading to a difference from the true absorption profile.

The key atomic physics is contained in the matrix element describing the probability of photon excitation, $M_{if} = \langle f|\exp(\mathrm{i}\boldsymbol{k}\cdot\boldsymbol{r})\boldsymbol{A}\cdot\boldsymbol{p}|\mathrm{i}\rangle$, where $\boldsymbol{k}$ is the photon wavevector, $\boldsymbol{r}$ is the electron position vector, $\boldsymbol{A}$ is the photon polarization vector and $\boldsymbol{p}$ is the electron momentum operator. It is usual to use the expansion $\exp(\mathrm{i}\boldsymbol{k}\cdot\boldsymbol{r}) \approx 1+\mathrm{i}\boldsymbol{k}\cdot\boldsymbol{r}-\frac{1}{2}(\boldsymbol{k}\cdot\boldsymbol{r})^2+\ldots$, and in the dipole approximation all terms but the first (unity) are discarded. This may be satisfied when $\boldsymbol{k}\cdot\boldsymbol{r} \ll 1$, typically appropriate for low photon energies (say $\leqslant$ 1.5 keV), although it is commonly assumed to be appropriate to much higher energies. In this dipole approximation the angular distribution of the total cross-section σ in a linearly polarized photon beam is

$$\frac{\mathrm{d}\sigma}{\mathrm{d}\Omega} = (\sigma/4\pi)[1+\beta(3\cos^2\theta-1)/2]$$

where θ is the angle between the photoelectron emission direction and $\boldsymbol{A}$. β is the asymmetry parameter which can take values between -1 and 2. Note that this expression is symmetric in the forward and backward photon propagation direction (which is perpendicular to $\boldsymbol{A}$). Going beyond the dipole approximation, one can include the second term in the expansion of $\exp(\mathrm{i}\boldsymbol{k}\cdot\boldsymbol{r})$ which leads to the magnetic dipole and quadrupole

contributions. The angular distribution can then be parametrized in the form [3]

$$\frac{d\sigma}{d\Omega} = (\sigma/4\pi)[1 + \beta(3\cos^2\theta - 1)/2 + (\delta + \gamma\cos^2\theta)\sin\theta\cos\phi]$$

introducing two additional asymmetry parameters δ and γ. ϕ is the angle between the photon propagation direction and the projection of the electron wavevector in the plane perpendicular to $\boldsymbol{A}$. It is the term containing this angle which introduces backward/forward asymmetry in the photoemitted signal relative to the photon propagation direction. If the electron detector lies in the plane defined by the photon incidence direction and the polarization vector $\boldsymbol{A}$, as in the experiments to be described, ϕ is equal to 0° when the electrons collected have a positive vector component in the direction of photon propagation ('forward') and 180° when this component is negative ('backward'). Note that when θ is 0° (electron emission perpendicular to the incidence direction and along the direction of the polarization vector $\boldsymbol{A}$), there is no contribution to the partial cross-section from the non-dipole terms.

To investigate the role of these multipole effects in XSW we have compared the effects of monitoring the x-ray absorption in an adsorbate atom both by Auger electron emission and by photoemission. We have also used two different detector geometries. In the first ('standard geometry') our concentric hemispherical electron energy analyser was mounted in its usual location at 40° to the incident photon direction (i.e. $\theta = 50^\circ$, $\phi = 180^\circ$; c.f. schematic in figure 1), while in a second series of experiments it was placed at 90° to the incidence direction ($\theta = 0^\circ$) ('dipolar geometry') such that any multipole contribution to the photoemission anisotropy should be lost.

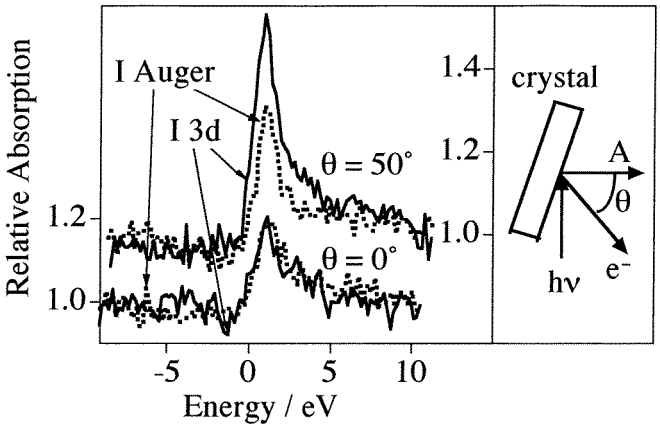

Figure 1. A schematic of the experimental geometry, defining the angle θ, is shown in the right-hand panel. On the left the relative intensities of the I 3d photoemission and I MNN Auger peaks from Cu(111)($\sqrt{3} \times \sqrt{3}$)R30°-I are compared as the incident x-ray energy is scanned through the normal incidence ($\bar{1}11$) Bragg condition for measurements in the 'standard' and 'dipole' collection geometries ($\theta = 50^\circ$ and $\theta = 0^\circ$ respectively). The scatter of the data points is consistent with statistical noise (see figure 2).

The specific system investigated was the Cu(111)($\sqrt{3} \times \sqrt{3}$)R30°-I adsorption phase. The NIXSW experiments used beamline 6.3 of the Synchrotron Radiation Source at Daresbury Laboratory which is fitted with a double-crystal (Ge(111)) monochromator and prefocussing mirror. The Cu(111) sample was prepared in the usual way by x-ray Laue alignment, spark machining, mechanical polishing and *in situ* Ar ion bombardment and

annealing until a clean well-ordered surface was obtained as indicated by low energy electron diffraction (LEED) and Auger electron spectroscopy. The I adsorption phase was prepared by thermal decomposition of a CdI_2 layer [10]. The experiments involved photon energy scans through the normal incidence (111) and ($\bar{1}$11) reflections from Cu at approximately 2975 eV, conducted respectively at normal incidence to the (111) surface and at 70.5° to the surface in the appropriate azimuth. The resulting two different local layer spacings deduced from the data allow us to triangulate the adsorbate site.

Measurements were made of the intensities of the Cu LVV Auger peak, the I MNN Auger peak, and the I $3p_{3/2}$ and I $3d_{5/2}$ photoemission peaks as the photon energy was scanned through these two NIXSW conditions. Using our standard NIXSW methodology [6] we first established the structural details of the adsorption structure from the experiment in the standard geometry using the Auger emission peaks which carry no memory of the initial photon direction and monitor the XSW amplitude directly. The Cu Auger signal was used as a monitor of the adsorption at the (known) bulk Cu sites, providing an absolute photon energy calibration, while the I Auger intensity profiles were fitted to obtain the two XSW structural parameters for the adsorbate, the coherent position and coherent fraction (see table 1 and figure 2). A previous surface-extended x-ray absorption fine structure (SEXAFS) study of this surface phase found the I atoms to occupy three-fold coordinated hollow sites at a Cu–I nearest-neighbour distance of 2.66 ± 0.02 Å, implying a Cu–I outer layer spacing of 2.21 ± 0.03 Å [11]. The XSW layer spacings are referenced to the nearest extended substrate scatterer plane, and our data clearly imply an outer layer spacing of one bulk layer spacing (2.08 Å) greater than the (111) coherent position (i.e. $1.03 \times 2.08 = 2.15 \pm 0.05$ Å), in good agreement with the SEXAFS value assuming no significant outer substrate layer spacing changes. The SEXAFS study [11] did not distinguish between the two different hollow sites lying above second ('hcp') or third ('fcc') substrate layer atoms. Based on the measured (111) layer spacing, the anticipated ($\bar{1}$11) coherent positions expected for these two sites are 0.67 and 1.01 respectively. The intermediate experimental value and the low ($\bar{1}$11) coherent fraction are consistent with mixed occupation of these sites [12].

While the I Auger electron signal provides a direct monitor of the x-ray absorption, the I photoemission signals will be influenced in the standard geometry by any multipole contribution to the excitation which introduces backward/forward asymmetry as described above. Confirmation that this is so for the I 3d photoemission is provided in figure 1 which compares the XSW profiles recorded from the I Auger and 3d photoemission signals around the ($\bar{1}$11) normal incidence reflection in the two different collection geometries. The amplitude of the XSW modulation is some 60% larger for the I 3d signal in the standard geometry, whereas the two signals are essentially identical with the detector in the 'dipolar geometry'. The I 3d signal in the standard geometry can be fitted in the usual way (e.g. figure 2), but the parameters obtained (table 1) differ significantly from the true values obtained from the Auger signal. Note, in particular, the coherent fraction for the (111) reflection which is greater than unity—a physically meaningless result. For the (111) NIXSW in the $\theta = 0°$ collection geometry, which involves the analyser axis lying in the plane of the surface, it was not possible to collect a usable signal from the 511 eV I Auger emission, but a noisy I 3d photoemission profile at the higher kinetic energy of around 2355 eV was obtained and could be fitted using structural parameter values similar to those obtained from fitting the I Auger signal in the standard geometry. By contrast to this behaviour for the I 3d signal, the 3p photoemission profiles were almost identical to those obtained from the I Auger signal in both geometries.

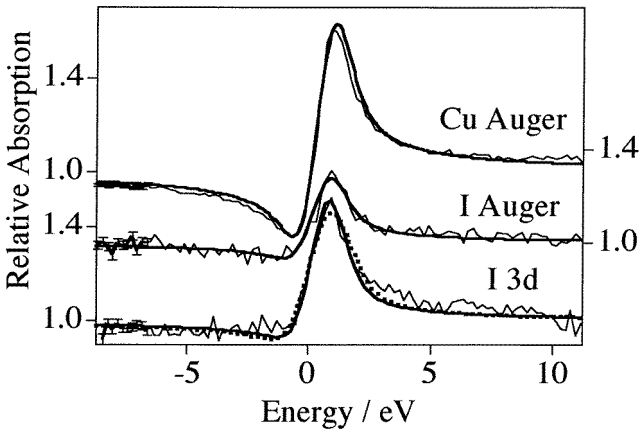

Figure 2. Theoretical fits (full lines) to the experimental data for the ($\bar{1}11$) NIXSW in the 'standard' geometry). Representative statistical error bars are shown superimposed on the first 10 data points of each spectrum. In the case of the I 3d photoemission data, two fits are shown, one (dashed line) neglecting the role of multipole excitations and fitting f_{co} and D, the other constraining these structural parameters to the values found by fitting the I Auger signal but allowing the multipole Q parameter to be optimized.

Table 1. Structural fitting parameter values obtained from NIXSW measurements in the standard collection geometry ($\theta = 50^\circ$) without multipole asymmetry correction. Estimated errors are based on the scatter found in fitting several different data sets.

		D/d_H	f_{co}
(111)	I MNN	0.03+0.02	0.81+0.05
	I 3d	0.06+0.02	1.21+0.05
($\bar{1}11$)	I MNN	0.89+0.02	0.44+0.05
	I 3d	0.04±0.02	0.42+0.05

In photoemission detection of the standing wave, the signal detected in a specific direction may be written as

$$\frac{\mathrm{d}\sigma}{\mathrm{d}\Omega}\alpha|\langle f|\exp(\mathrm{i}\boldsymbol{k}_0\cdot\boldsymbol{r})\boldsymbol{A}_0\cdot\boldsymbol{p}|\mathrm{i}\rangle + |E_H/E_0|\exp(\mathrm{i}(\phi - 2\pi\boldsymbol{H}\cdot\boldsymbol{r})) \times\langle f|\exp(\mathrm{i}\boldsymbol{k}_H\cdot\boldsymbol{r})\boldsymbol{A}_H\cdot\boldsymbol{p}|\mathrm{i}\rangle|^2$$

where the suffices 0 and H relate to the incident and reflected x-rays and $|E_H/E_0| = \sqrt{R}$ with R the x-ray (intensity) reflectivity, while ϕ defines the relative phase of this reflected wave. An evaluation of this expression for a general x-ray incidence angle to the scatterer planes in the dipole approximation has been given previously [8]. Here we consider only the case of normal incidence to the scatterer planes, but include the effects of non-dipole excitation in a simple parametrized fashion by a forward/backward asymmetry factor, Q, defined such that the ratio of the photoemission intensity for ϕ values of 0° and 180° at the θ value (50°) appropriate to the measurement is given by $(1 + Q)/(1 - Q)$. Evidently Q must fall in the range between -1 and $+1$; in the pure dipole case it is zero. Using this formalism one can separate out the key angular dependence components of the two matrix

elements in this equation to give

$$\frac{\mathrm{d}\sigma}{\mathrm{d}\Omega}\alpha|M(1-Q)^{1/2}+\sqrt{R}\exp(\mathrm{i}(\phi-2\pi\boldsymbol{H}\cdot\boldsymbol{r}))M(1+Q)^{1/2}|^2$$

where the remainder of the matrix element M contains all other aspects including the angular dependence relative to the polarization vector $\boldsymbol{A}$, which, being in the same direction for both incident and reflected waves in the NIXSW condition, is identical for both components. Expanding this expression, including the effects of a distribution of absorber layer spacings z relative to the scatterer planes of separation d_H [4, 5, 9] and normalizing to a value of unity for conditions far from the Bragg condition (when $R = 0$) gives

$$\frac{\mathrm{d}\sigma}{\mathrm{d}\Omega}\alpha[1+R(1+Q)/(1-Q)+2\sqrt{R}f_{co}((1+Q)/(1-Q))^{1/2}\cos(\phi-2\pi D/d_H)]$$

where D and f_{co} are the usual coherent position and coherent fraction respectively. Notice that for positive values of Q the apparent reflectivity and the amplitude of the interference term are enhanced relative to the zero Q (dipole) case. Analysing data for which Q is positive with the normal ($Q = 0$) XSW expression is thus likely to lead to an enhancement of the apparent value of the coherent fraction, f_{co}, exactly as we have found for the I 3d emission in our (111) NIXSW experiment.

Our I photoemission NIXSW scans have been re-analysed using this modified expression, taking the values of the coherent fraction and coherent position as determined from the I Auger electron emission data, but varying Q to optimize the fits (e.g. figure 2). This gave values of Q for the I 3p and I 3d signals of 0.03 ± 0.05 and 0.21 ± 0.05 respectively. There are no published theoretical values of the angular parameters for I, but values are available for Xe [3], adjacent in the periodic table, and these should provide a rather good estimate for I at similar photoelectron kinetic energies. The appropriate values of β, γ and δ are for the 3p photoemission 1.60, 0.08 and 0.01 and for the 3d emission 1.16, 0.53 and 0.10. For our experimental geometry these lead to forward/backward asymmetry values of 1.057 and 1.545 respectively, giving calculated Q values of 0.03 for the 3p emission and 0.21 for the 3d signal. These are clearly in excellent agreement with our experimental values.

In conclusion, our data show that non-dipole contributions to the angular dependence of photoemission can significantly influence the structural parameters deduced from normal incidence x-ray standing wave studies of surface structures at photon energies below 3 keV. However, we have shown that these effects are quantitatively consistent with theoretically calculated asymmetry factors in atomic physics, and that using these asymmetry factors in conjunction with a simple modified expression, photoelectron detection NIXSW can be used to obtain the correct structural parameters. A survey of the calculated asymmetry parameters for the inert gases [3] indicates that these effects will be important in many XSW studies; for example, for low atomic number elements such as C,N,O and F, but also for Al, Si and P, the quadrupole correction to the 1s emission will be substantial at the lowest ($\approx$ 3 keV) energies used in NIXSW, and is even more important at higher energies. Indeed, the effects are generally important for all comparably shallow binding energy states at these photon energies, but can also be important quite close to photoionization threshold for other states; in this regard our I 3p measurements fortuitously correspond to an energy at which γ passes through a minimum. A number of published NIXSW structure determinations will need reassessing in the light of these findings.

The authors acknowledge the support of this work in the form of beamtime awards from CCRLC Daresbury Laboratory and studentships for CJF and GJJ from the Engineering and Physical Sciences Research Council and for RI from the University of Malaya.

References

[1] Krassig B, Jung M, Gemmell D S, Kanter E P, LeBrun T, Southworth S H and Young L 1996 *Phys. Rev. Lett.* **75** 4736
[2] Jung M, Krassig B, Gemmell D S, Kanter E P, LeBrun T, Southworth S H and Young L 1997 *Phys. Rev.* A **54** 2127
[3] Cooper J W 1993 *Phys. Rev.* A **47** 1841
[4] Vartanyants I A and Zegenhagen J 1997 *Il Nuovo Cimento* D **19** 617
[5] Batterman B W and Cole H 1964 *Rev. Mod. Phys.* **36** 681
[6] Zegenhagen J 1993 *Surf. Sci. Rep.* **18** 199
[7] Woodruff D P, Seymour D L, McConville C F, Riley C E, Crapper M D, Prince N P and Jones R G 1987 *Phys. Rev. Lett.* **58** 1460
Woodruff D P, Seymour D L, McConville C F, Riley C E, Crapper M D, Prince N P and Jones R G 1988 *Surf. Sci.* **195** 237
[8] Sugiyama M, Maeyama S, Heun S and Oshima M, 1995 *Phys. Rev.* B **51** 14 778
[9] Berman L E and Bedzyk M J 1989 *Phys. Rev. Lett.* **63** 1172
[10] Ithin R and Jones R G 1996 *J. Phys.: Condens. Matter* **8** 3285
[11] Citrin P H, Eisenberger P and Hewitt R C 1980 *Phys. Rev. Lett* **45** 1948
[12] Woodruff D P, Cowie B C C, Ettema A R H F 1994 *J. Phys: Condens. Matter* **6** 10 633